

# UC San Diego

## UC San Diego Previously Published Works

### Title

Decrease of VEGF-A in myeloid cells attenuates glioma progression and prolongs survival in an experimental glioma model.

### Permalink

<https://escholarship.org/uc/item/3mb2677j>

### Journal

Neuro-oncology, 18(7)

### ISSN

1523-5866

### Authors

Osterberg, Nadja  
Ferrara, Napoleone  
Vacher, Jean  
[et al.](#)

### Publication Date

2016-07-01

### DOI

10.1093/neuonc/now005

Peer reviewed

## Decrease of VEGF-A in myeloid cells attenuates glioma progression and prolongs survival in an experimental glioma model

Nadja Osterberg, Napoleone Ferrara, Jean Vacher, Simone Gaedicke, Gabriele Niedermann, Astrid Weyerbrock, Soroush Doostkam, Hans-Eckart Schaefer, Karl H. Plate, and Marcia Regina Machein

Department of Neurosurgery, Freiburg University Medical School, Freiburg, Germany (N.O., A.W., M.R.M.); Department of Pathology, University of California San Diego, San Diego, California (N.F.); Department of Medicine, Institut de Recherches Cliniques de Montréal, Université de Montréal, Québec, Canada (J.V.); Department of Radiation Oncology, University Hospital Freiburg, Germany (S.G., G.N.); Department of Neuropathology, Freiburg University Medical School, Freiburg, Germany (S.D.); Department of Pathology, Freiburg University Medical School, Freiburg, Germany (H.-E.S.); Institute of Neurology (Edinger Institute), Frankfurt University Medical School, Frankfurt, Germany (K.H.P)

**Corresponding Author:** Marcia Regina Machein, MD, Neurocenter, Department of Neurosurgery, Freiburg University Medical School, Breisacher Straße 64, D-79106 Freiburg, Germany (marcia.machein@uniklinik-freiburg.de).

**Background.** Glioblastomas are highly vascularized tumors with a prominent infiltration of macrophages/microglia whose role in promoting glioma growth, invasion, and angiogenesis has not been fully elucidated.

**Methods.** The contribution of myeloid-derived vascular endothelial growth factor (VEGF) to glioma growth was analyzed in vivo in a syngeneic intracranial GL261 glioma model using a Cre/loxP system to knock out the expression of VEGF-A in CD11b + myeloid cells. Changes in angiogenesis-related gene expression profile were analyzed in mutant bone marrow-derived (BMD) macrophages in vitro. Furthermore, we studied the influence of macrophages on GL261 growth, invasiveness, and protein expression profile of angiogenic molecules as well as the paracrine effect of mutant macrophages on angiogenesis in vitro.

**Results.** Myeloid cell-restricted VEGF-A deficiency leads to a growth delay of intracranial tumors and prolonged survival. The tumor vasculature in mutant mice was more regular, with increased pericyte coverage. Expression analysis revealed significant down-regulation of VEGF-A and slight upregulation of TGF $\beta$ -1 in BMD macrophages from mutant mice. Endothelial tube formation was significantly decreased by conditioned media from mutant macrophages. The expression of angiogenesis-related proteins in GL261 glioma cells in co-culture experiments either with wild-type or mutant macrophages remained unchanged, indicating that effects observed in vivo are due to myeloid-derived VEGF-A deficiency.

**Conclusions.** Our results highlight the importance of VEGF derived from tumor-infiltrating myeloid cells for initiating vascularization in gliomas. The combination of antiangiogenic agents with myeloid cell-targeting strategies might provide a new therapeutic approach for glioblastoma patients.

**Keywords:** angiogenesis, glioma, macrophages, microglia, VEGF.

Glioblastoma is a highly invasive and angiogenic tumor with prominent vascularization. The vascular endothelial growth factor (VEGF) has been identified as a critical regulator of the angiogenic response in glioblastomas.<sup>1,2</sup> Encouraging results after antiangiogenic treatment were observed in preclinical glioblastoma models. However, clinical trials using antiangiogenic drugs, including VEGF blockage, showed that most human glioblastomas become resistant to anti-VEGF therapy after an initial temporary response. Growing evidence suggests that tumor progression and angiogenesis are supported by nontumor cells residing in the tumor microenvironment, in

particular members of the innate immune system.<sup>3,4</sup> CD11b<sup>+</sup> cells of myeloid lineage, such as tumor-associated macrophages (TAMs), Tie-2 expressing monocytes (TEMs), neutrophils, and myeloid-derived suppressor cells are present in the tumor microenvironment. In addition to infiltrating leukocytes, resident CD11b<sup>+</sup> microglia also contribute to glioma progression.<sup>5</sup> Upon hypoxia, chemo-attractants including VEGF mediate the recruitment of protumorigenic myeloid cells which themselves produce VEGF upon interaction with tumor cells.<sup>6</sup> An increase in TAMs after antiangiogenic therapy is associated with poor survival in patients with glioblastomas, and increase in neutrophil

Received 9 April 2015; accepted 11 January 2016

© The Author(s) 2016. Published by Oxford University Press on behalf of the Society for Neuro-Oncology. All rights reserved. For permissions, please e-mail: journals.permissions@oup.com.

infiltration is correlated with glioma grade and acquisition of resistance to anti-VEGF therapy.<sup>7</sup> In previous studies, we demonstrated that the elimination of VEGF receptor 1 (VEGFR-1) signaling in BMD cells significantly decreases glioma growth and vascularization in an experimental model, which suggests that myeloid cells expressing VEGFR-1 play a crucial role in initiating and sustaining glioma angiogenesis.<sup>8</sup> Furthermore, we showed that the expression of VEGF is decreased in myeloid cells lacking functional VEGFR-1.<sup>9</sup> These findings suggest that BMD myeloid cells are an important source of VEGF. The aim of this study was to investigate the relevance of myeloid cell-derived VEGF-A in glioma growth and vascularization by an orthotopic GL261 glioma model using transgenic mice deficient for VEGF-A in CD11b<sup>+</sup> myeloid cells.

## Materials and Methods

All animal experiments were carried out according to the approval of the local animal care committee concerning the use and care of experimental animals.

### Myeloid Cell Lineage Deletion of VEGF-A

The VEGF-A gene flanked by loxP sites (VEGF<sup>lox/lox</sup>) in C57BL6-background mice was obtained from Genentech.<sup>10</sup> Targeted deletion of VEGF-A in myeloid cells was achieved by crossing female transgenic mice with the loxP-flanked VEGF-A allele (VEGF<sup>lox/lox</sup>) with male mice expressing the Cre recombinase driven by the CD11b promoter (CD11bcre).<sup>11</sup> Genotyping of transgenic mice was performed on tail DNA. Primer information and genotyping are provided in supplementary data.

### Fluorescence-activated Cell Sorting Analysis of Bone Marrow Cells

Tissue-specific recombination was evaluated by crossing the CD11bcre mice with mice ubiquitously expressing the lox-STOP-lox-LacZ transgene (Rosa 26).<sup>12</sup> When Rosa 26 mice are crossed with a cre transgenic strain, LacZ is expressed in cells/tissues where cre is expressed. Recombination was evaluated by fluorescence-activated cell sorting (FACS) analysis of  $\beta$ -galactosidase ( $\beta$ -Gal) expression in CD11b<sup>+</sup> bone marrow cells.<sup>13</sup> Samples were examined using CellQuest software (Becton Dickinson).

### Detection of Cre-mediated Recombination of VEGF-A Exon 3

Detection of Cre-mediated recombination was performed on genomic DNA obtained from BMD macrophages as described earlier.<sup>14</sup> Briefly, the primer pair VEGF<sub>c5R.2</sub> and VEGF<sub>322.F</sub><sup>15</sup> were used for PCR to detect the complete excision of exon 3.

### In Vitro Generation of Bone Marrow-derived Macrophages

Bone marrow cells were obtained from mice by flushing the tibias and fibulas. Cells were differentiated into macrophages as previously described.<sup>16</sup> Characterization of the cells is described in Supplementary Data.

### ELISA for Mouse VEGF-A

The VEGF-A concentrations in the culture supernatants were assessed by ELISA. The method is described in Supplementary Data.

### Cell Line and Lentiviral Transduction

Murine glioma GL261 cells were kindly provided by Dr. Gaetano Finocchiaro (Istituto Nazionale Neurologico Carlo Besta, Milan, Italy).<sup>17,18</sup> Glioma cells were cultured in Dulbecco's modified Eagle's medium containing 10% fetal calf serum (FCS). Generation of GL261-luciferase is described in Supplementary data.

### RNA Isolation, Reverse Transcription, Angiogenesis PCR Array, and Quantitative Real-time PCR

RNA extraction was performed using the Qiagen RNA mini kit according to the manufacturer's instructions. RNA isolation from intracranial tumors was performed as described previously.<sup>8</sup>

The expression profile of angiogenesis-related genes in BMD macrophages obtained from CD11bcre + VEGF-A<sup>+/+</sup> mice (control) in comparison with those retrieved from CD11bcre + VEGF-A<sup>loxP/loxP</sup> mice was analyzed using the RT2 Profiler PCR Array for Mouse Angiogenesis (PAMM-024; SABiosciences). Further information is available in Supplementary Data.

### Western Blot Analysis

Conditional media (CM) from in vitro differentiated macrophages were collected after 24 hours, centrifuged for 10 minutes at 3000 rpm, and concentrated (Centricon, 10 kDa, Amicon). Total BMD macrophage lysates or equal amounts of concentrated CM were subjected to SDS-PAGE and transferred to polyvinylidene difluoride (PVDF) membranes. The following primary antibodies were used: rabbit anti-mouse TGF $\beta$ -1, rabbit anti-mouse HIF-1 $\alpha$  (Novus Biologicals), goat anti-mouse VEGFB167/187, goat anti-mouse PlGF-2 (R&D), and goat anti-b-actin (Santa Cruz Biotechnology). After incubation with primary antibodies and proper secondary antibodies, detection was performed by chemiluminescence (Fisher Scientific).

### Endothelial Tube Formation Assay

BMD macrophages obtained from control and VEGF-A mutant mice were cultured until 70% confluence. After serum starvation (1%), the medium was conditioned for 48 hours. The supernatant was collected, and its ability to promote tubular structures in vitro was evaluated using the tube formation assay as described in Supplementary Data.

### Tumor Implantation

For the tumor implantation studies, we used age-matched male mutant (CD11bcre + VEGF-A<sup>loxP/loxP</sup>) and control (CD11bcre + VEGF-A<sup>+/+</sup>) mice. Wild-type (WT) GL261 or GL261-LUC/GFP cells ( $0.8 \times 10^5$ ) were slowly inoculated intracerebrally into the right caudate nucleus as previously described.<sup>8</sup>

### Tumor Volume Analysis

For tumor volume analysis, mice were euthanized through cardiac perfusion 18 days after tumor implantation. The tumor volume was evaluated as described in Supplementary Data.

### Kaplan–Meier Survival Analysis of Mice With Orthotopic Malignant Glioma

Mice were intracranially implanted with GL261-LUC/GFP cells. Routine general health evaluation was conducted daily. Mice with signs of tumor burden were euthanized. Brains were isolated and processed for immunohistochemical evaluation. In vivo bioluminescence imaging was performed as described in Supplementary Data.

### Immunofluorescence

Immunofluorescence on PFA-fixed 50  $\mu$ m vibratome sections (VT-1000S; Leica Microsystems) was performed using the following antibodies: anti-mouse platelet-derived growth factor receptor- $\beta$  (PDGFR- $\beta$ ), anti-mouse CD140b (eBioscience), anti-human von Willebrand factor (vWF; DAKO), anti-mouse F4/80 (Serotec) as previously described.<sup>8</sup> Sections were analyzed with a krypton-argon laser scanning confocal imaging system (TCSNT, Leica Microsystems).

### Vessel Density and Vessel Maturation Index

Sections were immunostained with vWF and PDGFR- $\beta$  antibodies. Confocal microscopy images of random tumor spots were taken at 40 $\times$  magnification. Morphometrical analysis is described in Supplementary Method Data.

### MTT (3-(4,5-Dimethyl-2-thiazolyl)-2,5-diphenyl-2H-tetrazoliumbromid) Cell Viability Assay

Cell viability of GL261 cells was assessed by MTT viability assay. Further information is available in Supplementary Data.

### Invasion Assay

The in vitro invasive ability of GL261 cells after TGF $\beta$ -1 treatment or the inhibition of TGF $\beta$  signaling was assessed using the transwell modified Boyden chamber method (description in Supplementary Method information).

### GL261 Glioma Cell/macrophage Co-culture and Mouse Angiogenesis Antibody Array

Changes in expression of angiogenesis-related proteins in GL261 cells induced by co-cultured WT and mutant macrophages were assayed by Mouse Angiogenesis Antibody Array (R&D). Further information is available in Supplementary Data.

### Histological Analysis of Human Glioblastomas

Formalin-fixed, paraffin-embedded samples of 6 surgical specimens from patients with primary diagnosis of glioblastoma (submitted for resection at the Department of Neurosurgery Freiburg) were evaluated. Informed written consent was obtained to use tumor tissue for analysis. Retrieval and scientific

analysis of patient-derived tissue was approved by the local ethics committee under protocol 100020/09. Immunostaining of human samples was performed as described in Supplementary Data.

### Statistical Analysis

Statistical analysis was performed with GraphPad (InStat) or SPSS Statistic 20 software. Survival analysis was performed using the Kaplan–Meier method. The relationship between recombination levels and VEGF-A protein levels in CM was determined using a nonparametric Spearman rank correlation. All other data were compared using an unpaired 2-tailed Student *t* test. Data were expressed as mean  $\pm$  SEM; *P* < .05 was considered as statistically significant.

## Results

### Characterization of Double Transgenic CD11bcre + VEGF-A<sup>loxP/loxP</sup> Mice

CD11bcre + male and VEGF-A<sup>loxP/loxP</sup> female mice were mated. The offspring were used in crosses to generate the following transgenic mice: CD11bcre + VEGF-A<sup>+/loxP</sup> and CD11bcre + VEGF-A<sup>loxP/loxP</sup>. In total, 232 mice were genotyped. CD11bcre + VEGF-A<sup>+/+</sup> mice were used as WT control. Cre-specific primers detected the presence of the *cre* transgene in male mice since transgene integration is in the Y chromosome in these mice. Primers that flank the loxP1 insertion site distinguish VEGF-A<sup>loxP/loxP</sup> homozygotes (150 bp) from VEGF-A<sup>loxP/+</sup> heterozygotes (100 and 150 bp) and VEGF-A<sup>+/+</sup> mice (100 bp) (Fig. 1A).

Recombination and successful excision of VEGF-A exon 3 were tested by amplification of DNA from BMD macrophages with primers flanking VEGF-A exon 3. PCR amplification disclosed a partial excision of VEGF-A exon 3 in the CD11bcre + VEGF-A<sup>loxP/loxP</sup> mice (2.1 kb for the WT, 560 bp for the mutant, Fig. 1B). VEGF-A protein levels were detected in the supernatant of BMD macrophages using a sensitive VEGF-A ELISA assay. VEGF secretion was significantly reduced in heterozygous and homozygous mice in comparison with WT mice but was not completely abolished (Fig 1C). The levels of recombination correlated with the VEGF-A protein levels (Spearman rank correlation = 0.791, *P* = .01; data not shown). Cell-type specific Cre expression was verified by mating CD11bcre mice to the Rosa26 mouse line, which ubiquitously expresses  $\beta$ -Gal. Transgene expression was evaluated in the bone marrow compartment and in the spleen by FACS analysis. Quantification of CD11b- and  $\beta$ -Gal-positive cells in the bone marrow compartment showed an efficiency of recombination of around 40%, demonstrated by the presence of 24% of CD11b<sup>+</sup>/LacZ<sup>+</sup> cells compared with 37% CD11b<sup>+</sup>/LacZ<sup>-</sup> cells. In the spleen, the level of CD11b<sup>+</sup>/ $\beta$ -Gal-positive cells was around 4% (Fig. 1D).

### Glioma Growth Is Inhibited in Homozygous CD11bcre + VEGF-A<sup>loxP/loxP</sup> Mice

To test the role of myeloid-derived VEGF in glioma angiogenesis and tumor development, we implanted syngeneic tumor cells intracranially into male transgenic mice. The mice were euthanized 18 days after tumor implantation, and the total tumor

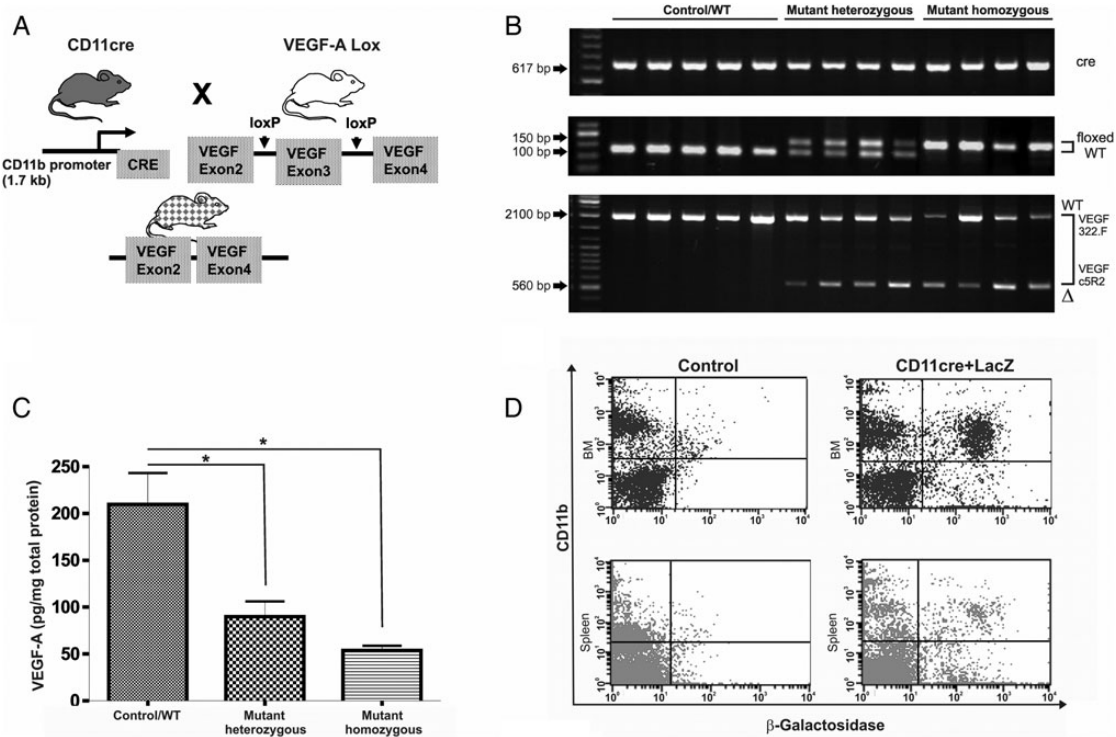


**Fig. 1.** Characterization of CD11cre + VEGF<sup>lox/lox</sup> mice. (A) Schematic diagram of the transgenic mice used to generate mutant CD11cre + VEGF<sup>lox/lox</sup>. (B) Mice genotyping: a band of 617 bp indicates the presence of cre transgene (top panel). A 100 bp band indicates wild-type (WT) VEGF-A allele; a 150 bp band corresponds to homozygous floxed VEGF-A (mutant homo VEGF<sup>lox/lox</sup>) allele. Heterozygous mice showed 100 bp and 150 bp bands (mutant hetero VEGF<sup>+/lox</sup>) (middle panel). PCR amplification of genomic DNA from bone marrow-derived (BMD) macrophage preparations with primers that bind to either side of VEGF-A exon 3 demonstrate the partial excision of this stretch of DNA. (A band of 2.1 kb represents wild-type VEGF-A<sup>+/+</sup>, and a band of 560 bp represents mutant mice (bottom panel). (C) Detection of VEGF-A in supernatants of cultured BMD-macrophages (control  $n = 9$ ; mutant hetero  $n = 4$ ; mutant homo  $n = 5$ ). Bars represent means and  $\pm$  SEM, (\* $P < .05$ ) (D) Quantification of expression of LacZ reporter driven by the CD11cre promoter in bone marrow and spleen cells derived from CD11cre + LacZ mice. Fluorescence-activated cell sorting (FACS) analysis disclosed that 40% of the CD11b<sup>+</sup> cells in bone marrow expressed the reporter gene. Low levels of recombination were detected in spleen macrophages.

was histologically evaluated. Control mice ( $n = 12$ ) had a mean tumor volume of 25.75 mm<sup>3</sup> (SEM = 4.46  $\pm$  15.45), whereas the mutant mice ( $n = 12$ ) had a mean tumor volume of 4.85 mm<sup>3</sup> (SEM = 2.12  $\pm$  7.36), showing a statistically significant difference between the tumor volumes in control versus mutant mice ( $P = .0010$ ) (Fig. 2A and B). We observed that 3 mice in the mutant group developed tumors with sizes similar to the control, and one animal in the control group had only a very small tumor. Although we used sex- and size-matched mice, we observed an intervariability in the tumor volume in both groups. To exclude these differences being due to technical problems during implantation, we performed a survival analysis using GL261-LUC/GFP cells. We monitored the bioluminescence signals on days 1 and 7 post tumor implantation. Mice without a detectable bioluminescence signal were excluded from the survival analysis (2 mice in the control group and one mouse from the mutant group died during bioluminescence analysis). Bioluminescence signals were similar at day 1 post implantation in both groups. The mean survival of the remaining control mice ( $n = 6$ ) was 22 days, whereas the mutant mice ( $n = 7$ ) had a significantly prolonged survival (mean 39 days) ( $P < .05$ ) (Fig. 2C and D). However, among the mutant

mice, 2 mice developed symptoms and were euthanized at day 23 and day 25 post implantation, similar to the control group. The tumors retrieved from these 2 mice disclosed a more irregular tumor border, with glioma cells surrounding the brain microvessels at a longer distance (Supplementary Material, Fig. S2) compared with the tumors developed in the control mice.

### Expression of Angiogenic Genes in Control and Mutant BMD Macrophages

To gain further insights into the mechanism by which CD11b<sup>+</sup> cells support glioma angiogenesis, we analyzed the gene expression profile of BMD macrophages using a PCR Mouse Angiogenesis Array (SABiosciences). The vast majority of genes did not show any significant changes. TGF $\beta$ -1 and MMP19 were found to be more than 5-fold upregulated, whereas VEGF-A and HIF-1 $\alpha$  were more than 5-fold downregulated (Fig. 3A). To verify this differential gene expression, we performed quantitative real-time PCRs using primer sets different from those used in the array. By this approach, we could confirm that only VEGF-A (5-fold downregulation)

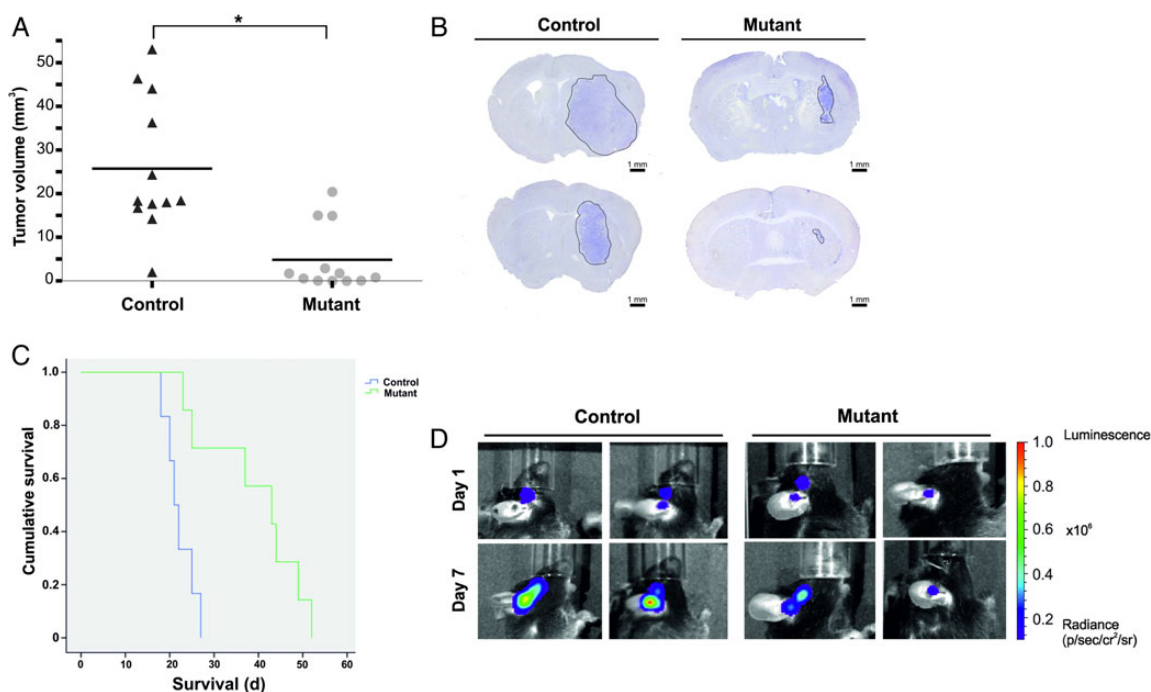


**Fig. 2.** Myeloid-derived VEGF-A plays an important role in glioma growth. (A) Analysis of tumor volumes in control (CD11bcre + VEGFA<sup>+/+</sup>) and in mutant (CD11bcre + VEGF<sup>lox/lox</sup>) mice. Results for individual animals are present. The bold lines represent the mean in each group (\* $P < .05$ ). (B) Representative images of brain section of intracranial tumor-bearing mice. Mice were euthanized at day 18 post tumor implantation. Sections (50  $\mu$ m) were stained with hematoxylin. Scale bar = 1 mm. (C) Kaplan-Meier survival analysis of mice implanted with GL261 stably expressing luciferase showing the prolonged survival of mutant mice. (D) Localization of bioluminescence (BLI) signal at day 1 and day 7 post implantation of GL261 expressing luciferase. Representative BLI scans show the anatomical injection site.

(Fig. 3B) and TGF $\beta$ -1 (3-fold upregulation) (Fig. 3C) were differentially expressed at a significant level. At the protein level, we confirmed the decreased expression of VEGF-A (Fig. 1C). Western blot analysis revealed that expression of TGF $\beta$ -1 protein was only slightly increased (1.5-fold,  $n = 3$ ) (Fig. 3D). PlGF-2 and VEGF-B were not detectable in cell lysates or in CM from unstimulated in vitro differentiated macrophages. Therefore, only VEGF-A expression was significantly down-regulated at the mRNA and protein level in mutant BMD macrophages.

VEGF-A mRNA levels in tumor tissue did not show significant differences between the 2 groups (data not shown). The VEGF-A mRNA levels in unstimulated macrophages were 2-fold higher than in unstimulated GL261 cells (data not shown).

#### Paracrine Influence of CD11b<sup>+</sup> Cells on Angiogenesis in Vitro

We examined the efficacy of CM obtained from BMD macrophages for inducing endothelial cell proliferation and the formation of a network of interconnecting tubule-like structures in vitro (Fig. 4A). Supernatants from CD11bcre + VEGF-A<sup>loxP/loxP</sup> mice induced a lower number of tube networks with a reduced number of branches and loops compared with the WT-BMD macrophages (Fig. 4B). The total tube length was significantly decreased when endothelial cells were incubated

with CM from VEGF-A mutant macrophages, similar to the endothelial cells incubated with medium containing 1% FCS alone (Fig. 4C).

#### Tumors in Mutant Mice Disclose Increased Vessel Normalization

We next examined the vascular network in intracranial gliomas. The tumor vasculature of the control groups was immature, with large chaotic vessels showing abundant sprouting and fewer pericytes closely associated to the blood vessels (Fig. 5A and C). The tumor vasculature in mutant mice was more regular, with less branching and diameter variation (Fig. 5B and D). The decrease in myeloid-derived VEGF-A resulted in a 40% reduction in vascular density (not statistically significant, Fig. 5G) and an increase in the level of pericyte coverage ( $P < .05$ , Fig. 5H). The levels of infiltration of macrophages (F4/80-immunopositive) into the intracranial gliomas were similar in all groups and were not influenced by the loss of VEGF-A in myeloid cells (Fig 5E, F and I).

#### Functional Blockage of TGF $\beta$ -1 in CM of Mutant Mice Decreases Invasiveness of GL261 Cells in Vitro

We further analyzed whether the differential expression of TGF- $\beta$ 1 in mutant macrophages have a functional significance in the proliferation, viability, and invasiveness of GL261 cells in

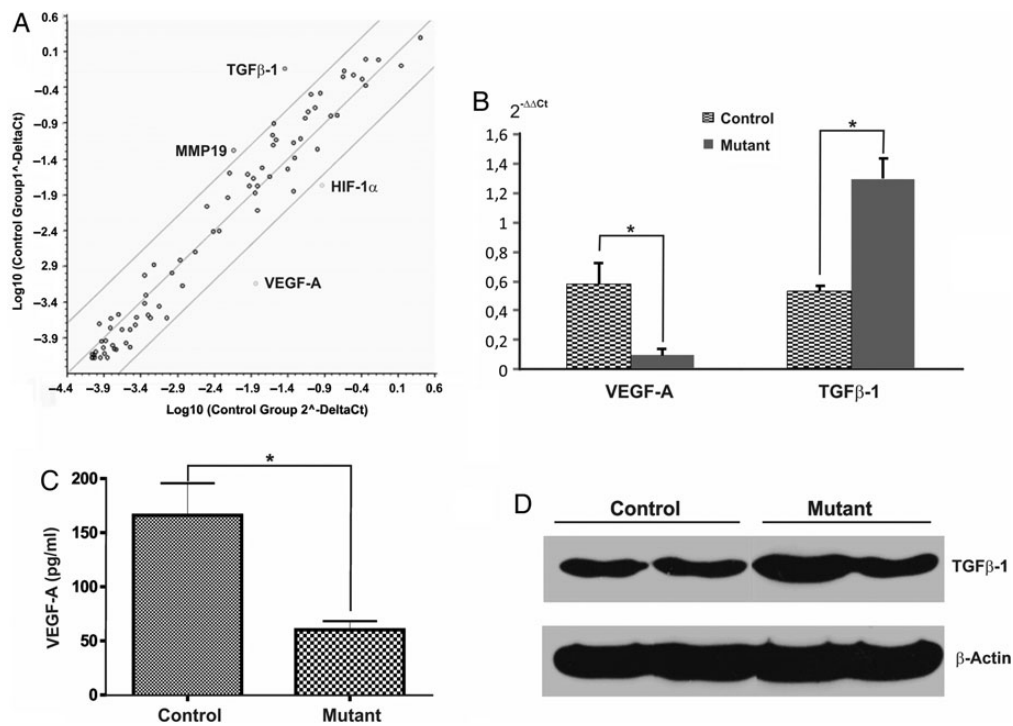


**Fig. 3.** Gene expression profile of in vitro differentiated macrophages. (A) Plot of a panel of 84 angiogenesis-related genes with a fold-change boundary  $>5$ . The differential expression of in vitro differentiated macrophages derived from control versus mutant mice ( $n = 4/\text{group}$ ) was evaluated using the RT2 Profiler Array System.  $\text{VEGF-A}$  and  $\text{HIF-1}\alpha$  were downregulated, whereas  $\text{MMP19}$  and  $\text{TGF}\beta-1$  were upregulated. (B) Validation of PCR array screening using real-time PCR confirmed the differential regulation of  $\text{VEGF-A}$  and  $\text{TGF}\beta-1$  at mRNA levels. (C)  $\text{VEGF-A}$  ELISA of supernatants from control and mutant macrophages confirms that  $\text{VEGF-A}$  protein in mutant macrophages was significantly decreased but not abolished. Bars represent means  $\pm$  SEM, ( $*P < .05$ ). (D) Representative Western blot analysis of  $\text{TGF}\beta-1$  protein expression in bone marrow-derived macrophages. Densitometric quantification of 3 independent experiments revealed a 1.5 increase of  $\text{TGF}\beta-1$  in mutant macrophages.

vitro. Cell viability of GL261 cells was not affected by CM of WT or mutant macrophages with or without recombinant  $\text{TGF}\beta-1$  (Supplementary Material, Fig. S3A). Incubation with CM derived from mutant macrophages did not affect the growth of GL261 in vitro compared with CM derived from WT macrophages (data not shown). Functional blocking of  $\text{TGF}\beta-1/2/3$  by a pan-specific antibody had no influence on cell viability either, whereas blocking the signal transduction via  $\text{TGF}\beta$  type I receptors (ALK4, ALK5, and ALK7) significantly reduced the cell viability of GL261 cells in CM of WT and mutant macrophages. This reduction was slightly stronger in GL261 cells cultured in CM WT. The invasion capacity of GL261 remained unaffected by CM from WT or mutant macrophages (Supplementary Material, Fig. S3B). Adding  $\text{TGF}\beta-1$  to the medium increased the number of invading cells only in WT CM. Interestingly, the functional blocking of  $\text{TGF}\beta-1/2/3$ , as well as blocking  $\text{TGF}\beta$  receptor type I by SB505124, had significantly stronger effects on GL261 cell cultured in CM of mutant macrophages. Expression analysis of angiogenesis-related proteins in GL261 cells co-cultured with WT or mutant macrophages using Mouse Angiogenesis Antibody-Array disclosed no major differences in the expression profile of angiogenic proteins (Supplementary Material, Fig. S3C). Thus, the reduction of tumor growth observed in mutant mice is most probably due to the intrinsic myeloid cell  $\text{VEGF-A}$  deficiency.

### Macrophages Express VEGF in Human Glioblastoma and Accumulate in Areas of Increased Vessel Proliferation

To study the clinical relevance of our experimental data, we analysed the expression and cellular localization of VEGF related to inflammatory cells (stained for CD68, Fig. 6A and B and for CD14, Fig. 6C) and to the tumor vasculature (stained for CD34, Fig. 6F). Surgical specimens were reviewed by a pathologist (H.E.S.) and a neuropathologist (S.D.). VEGF protein was localized in tumor blood vessels (Fig. 6D and E) as well in areas with increased accumulation of  $\text{CD14}^+$  and  $\text{CD68}^+$  cells. Serial sections disclosed the expression of VEGF in CD68-positive macrophages often surrounding small blood vessels highlighted by a positive endothelial signal for CD34. Thus, besides hypoxic tumor cells, tumor-infiltrating macrophages in human glioblastoma are a source of  $\text{VEGF-A}$ .

### Discussion

In the current study, we examined whether conditional inactivation of  $\text{VEGF-A}$  in myeloid cells affects glioma growth in an intracranial syngeneic glioma model. We provide evidence that glioma development and growth are supported by  $\text{VEGF-A}$  provided by myeloid cells. The clinical relevance of our experimental findings is supported by the fact that myeloid

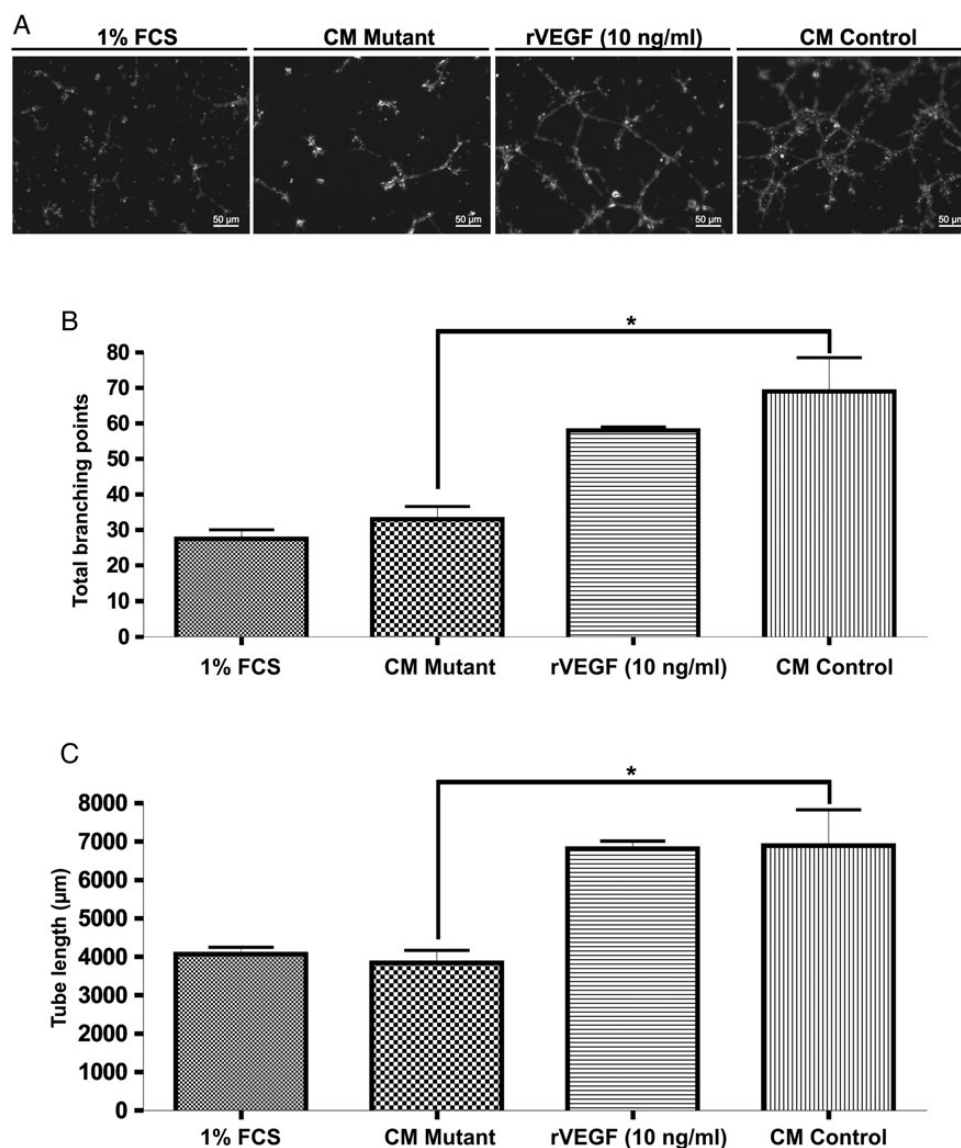


**Fig. 4.** Decreased VEGF-A expression by macrophages inhibits tube formation in vitro. (A) Representative images of Matrigel tube formation assay after a 12 hour incubation. Rat brain endothelial cells were incubated with conditioned media from control and mutant macrophages. Media containing 1% FCS and recombinant mouse VEGF-A were used as control. The graphs display total branching points (B) and the total tube length (C) (2 samples/group). Bars represent means  $\pm$  SEM, (\* $P < .05$ ).

cells in human glioblastomas express VEGF-A. Myeloid cells have been suggested to “kick-start” the angiogenic switch in early stages of tumor development, being the initial source of VEGF, perhaps even before tumor cells themselves start the secretion of VEGF.<sup>19</sup> Microglial CD11b<sup>+</sup> cells play a dominant role in the early stages, whereas the CD11b<sup>+</sup> infiltrating macrophages derived from circulating monocytes are major participants in the later stages of glioma growth; moreover, other CD11b<sup>+</sup> cells such as neutrophils are abundant in gliomas and have tumor-trophic activities.<sup>20</sup> The angiogenic switch is characterized by formation of a high-density vascular network essential for exponential tumor growth. Among the cellular triggers of this process, VEGF-A has a critical role.<sup>21</sup> Lin et al<sup>22</sup> showed that genetic ablation of macrophages in mammary

tumors delayed the angiogenic switch and that VEGF-A alone is sufficient to promote angiogenesis and to compensate for the deficiency of macrophages.<sup>23</sup> In this study, we observed that glioma growth in mice with reduced myeloid-derived VEGF-A was delayed. At day 18, mutant mice had barely detectable intracranial tumors compared with the control group. In a further experimental setting, we observed that the survival of mutant mice bearing intracranial tumors was significantly longer compared with control mice. This highlights the importance of VEGF-A derived from nontumor cells. Indeed, previous studies have shown that blocking human tumor-derived VEGF-A alone is not sufficient to inhibit tumor growth since host-derived VEGF-A compensates for the lack of tumor-derived VEGF-A.<sup>24</sup> We previously showed that VEGFR-1



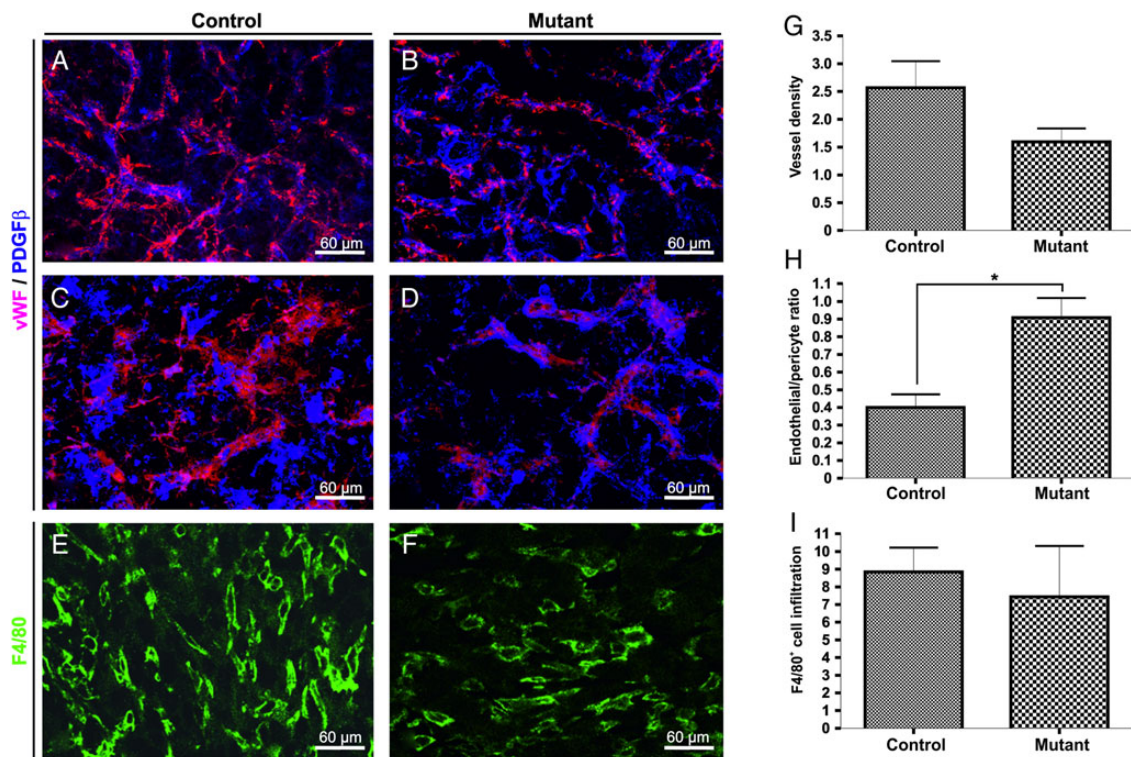


**Fig. 5.** Normalization of the tumor vasculature gliomas grown in mutant mice. Representative confocal microscopy images of double immunofluorescence for von Willebrand's factor (vWF; detection of endothelial cells, red) and PDGFR $\beta$  (detection of pericytes, blue) showing the vascular network in intracranial gliomas from control (A and C) and mutant animals (B and D). Quantitative analysis of vascular density (G) and pericyte cover index (H) in the different groups ( $n = 3-5$  animals/group). Representative confocal images of macrophage infiltration determined by staining with F4/80 in control (E) and mutant (F) tumors. Quantification analysis shows no substantial difference in the accumulation of inflammatory cells in mutant tumors compared with control tumors (I). Scale bar = 30  $\mu\text{m}$ . Bars represents means  $\pm$  SEM, (\* $P < .05$ ).

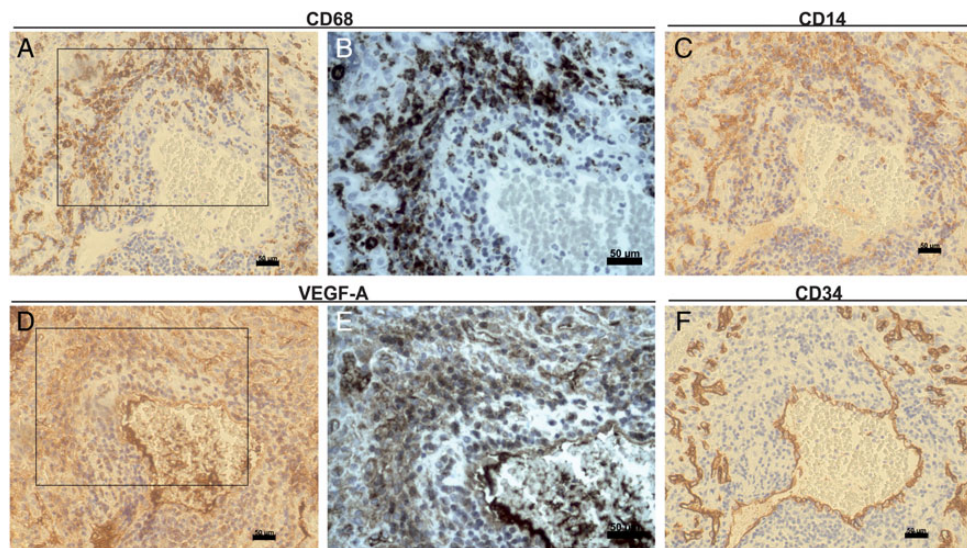


**Fig. 6.** Infiltrating tumor macrophages are a source of VEGF in human glioblastomas. Human glioblastoma serial sections were stained immunohistochemically with anti-VEGF (D and E) anti-CD68 (A and B), anti-CD14 (C), and anti-CD34 (F). High magnification of boxed areas is shown in B and C. Both tumor cells and macrophages produce VEGF in glioblastomas. VEGF protein is found on endothelial cells of CD34 + tumor vessels and particularly in perivascular CD68 + macrophages. Scale bar 50  $\mu\text{m}$ .

signaling in BMD-infiltrating cells plays an essential role in glioma development as loss of VEGFR-1 signaling in BMD myeloid cells leads to a significant decrease in tumor volume and vascularization. Tumor growth could be restored when VEGF is overexpressed by glioma cells. In line with our previous results, the experimental data presented here support the concept that VEGF-A from both tumoral and myeloid cells promotes glioma growth in an additive manner. Of importance, the total VEGF-A mRNA amounts from tumors retrieved from control and transgenic mice at the time of symptom development did not show major differences between the 2 groups, suggesting that VEGF-A derived from myeloid cells might be important in the early phases of glioma growth, but tumor cells are the prevailing source of VEGF at later stages.

Some mutant mice in both experiments developed tumors bigger than those observed in the control group. This might be related to the partial Cre-mediated excision in the myeloid compartment and the fact that the amount of VEGF in BMD macrophages retrieved from CD11bcre + VEGF<sup>loxP/loxP</sup> was significantly diminished but not abolished.

Furthermore, we observed a more invasive growth pattern in mutant mice. Baker et al<sup>25</sup> showed that gliomas might grow in a VEGF- and angiogenesis-independent vascularization manner by a process denominated “brain tumor autovascularization”. In this process, the tumor mass is vascularized by pre-existing brain tumor microvessels due to invasive glioma cells entering perivascular channels at the tumor border. Clinical and experimental data suggest that VEGF depletion leads to a proinvasive phenotype of malignant glioma. This might be a possible mechanism by which human gliomas escape antiangiogenic therapies, explaining why anti-VEGF therapy alone is ineffective in patients with glioblastoma.<sup>26</sup>

We next addressed whether the decrease in intrinsic VEGF-A production affects the gene expression of myeloid cells and induces myeloid cells to secrete alternative proangiogenic cytokines. We observed in BMD macrophages the expected downregulation of VEGF-A mRNA and a 3-fold upregulation of TGF $\beta$ -1. The amount of TGF $\beta$ -1 protein was, however, only slightly augmented (1.5-fold) in mutant macrophages. In vitro studies using CM of WT and mutant macrophages did not show any effect on the viability or proliferation of GL261 cells. Incubation with the receptor type I inhibitor SB505124 GL261 cell viability was reduced in both groups at similar levels. Interestingly, the invasion capacity of GL261 cells after blocking TGF $\beta$  signal transduction or its neutralization using specific antibody in CM of mutant macrophages was significantly reduced compared with WT CM. Thus, we speculate that TGF $\beta$ -1 might contribute to the invasive tumor growth pattern in mutant mice. In line with these findings, a recent study has shown the association between macrophage/microglia-derived TGF $\beta$ -1 and the increased invasive behavior of cancer stem cells in murine gliomas.<sup>27</sup> Of importance, screening with an antibody protein array disclosed no differences in expression profile of angiogenic proteins in GL261 after co-cultivation with mutant macrophages. Using Western blot, we could not detect VEGF-B or PlGF-2 protein in unstimulated macrophages.

In our study, the decrease of VEGF of CD11b<sup>+</sup> infiltrating cells is associated with an increased pericyte-coverage index. In vitro, the ability of endothelial cells to form tubular structures when incubated with CM of mutant macrophages is

reduced. This observation is in line with the well-established role of VEGF provided by infiltrating macrophages as an inducer of the angiogenic response and a negative regulator of vessel maturation and pericyte function.<sup>28,29</sup>

Our data contradict those of Stockmann et al<sup>30</sup> who reported that lineage-specific targeted deletion of VEGF in myeloid cells accelerates tumor growth in subcutaneous tumor models of lung cancer and in a spontaneous transgenic model of breast cancer. The authors showed that the vascular network is more organized in the absence of myeloid cell-derived VEGF, with an increased level of pericyte coverage that might be responsible for the accelerated tumor progression. We have previously shown that the infiltration of BMD leukocytes is substantial in GL261 gliomas; therefore, in comparison with other tumor types, the contribution of these cells to the total amount of VEGF in the tumor is correspondingly significant. Another possible explanation is the difference in the transgenic models used to induce myeloid cell gene ablation. In the experiments conducted by Stockmann et al,<sup>30</sup> LysM Cre knock-in mice were used to create a lineage-specific target deletion, whereas in our study we employed a Cre recombinase under the control of the CD11b promoter, thus possibly targeting different subpopulations of myeloid cells. Previous experiments using the LysM Cre recombinase showed low recombination efficacy in microglia.<sup>32</sup> Furthermore, the heterogeneous population of myeloid cells does not respond uniformly to microenvironmental changes.<sup>33,34</sup> Recent studies have focused on the pleiotropic activity of tumor-infiltrating myeloid cell subpopulations, particularly referring to the angiogenic process. Tissue macrophages, expressing the angiogenic receptors Tie-2 and neuropilin-1 but lacking LysM, differ phenotypically and functionally from monocyte-derived TAMs. Tie-2-expressing macrophages have been implicated as critical cellular chaperones for the formation of vascular anastomoses, whereas BMD macrophages provide a significant source of VEGF.<sup>35</sup> Gabrusiewicz et al<sup>36</sup> demonstrated that glioma growth is accompanied first by an accumulation of microglia (Iba-1<sup>+</sup>/CD11b<sup>+</sup>/CD45<sup>low</sup>), followed by infiltration of blood-derived macrophages (CD11b<sup>+</sup>/CD45<sup>high</sup>). Moreover, they showed that treatment of glioma-bearing animals with cyclosporine attenuated microglia/macrophage infiltration and reduced intracranial tumor growth. Using mice expressing the herpes simplex virus thymidine kinase under the control of the CD11b promoter, Zhai et al<sup>5</sup> reported that local ablation of microglia/macrophages decreased the intracranial glioma size and prolonged the survival of ganciclovir-treated mice. However, using the same approach, Galarneau et al<sup>37</sup> demonstrated that macrophage depletion after ganciclovir treatment resulted in a 33% increase in tumor volume. These controversial studies underline the phenotypic and functional complexity of the microglia/macrophage functions in glioma growth.

Although further experimental data are required to dissect the mechanisms by which myeloid cells affect glioma growth, our results highlight the role of myeloid-derived VEGF-A to timely induce the formation of an abnormal vascular network, promote glioma growth, and support the recent notion that microglial cells as well as myeloid cells represent a target in glioblastoma therapy. The combination of antiangiogenic agents with myeloid cell-targeting strategies might provide a new therapeutic approach for glioblastoma patients.

## Supplementary Material

Supplementary material is available at *Neuro-Oncology* online (<http://neuro-oncology.oxfordjournals.org/>).

## Funding

This study was supported by the Deutsche Krebshilfe (no. 109410; M.R.M. and K.H.P).

## Acknowledgments

We thank See Kwun Wong, Thomas Lutz, Nicole Rupp, Isabel Bahm, and Christine El Gaz for genotyping the different mouse strains and for their technical assistance.

*Conflict of interest statement.* None declared.

## References

- Machein M, de Miguel LS. Angiogenesis in gliomas. *Recent Results Cancer Res.* 2009;171:193–215.
- Machein MR, Plate KH. VEGF in brain tumors. *J Neurooncol.* 2000; 50(1–2):109–120.
- Allavena P, Mantovani A. Immunology in the clinic review series; focus on cancer: tumour-associated macrophages: undisputed stars of the inflammatory tumour microenvironment. *Clin Exp Immunol* 2012;167(2):195–205.
- Mantovani A, Germano G, Marchesi F, Locatelli M, Biswas SK. Cancer-promoting tumor-associated macrophages: new vistas and open questions. *Eur J Immunol.* 2011;41(9):2522–2525.
- Zhai H, Heppner FL, Tsirka SE. Microglia/macrophages promote glioma progression. *Glia* 2011;59(3):472–485.
- Harmey JH, Dimitriadis E, Kay E, Redmond HP, Bouchier-Hayes D. Regulation of macrophage production of vascular endothelial growth factor (VEGF) by hypoxia and transforming growth factor beta-1. *Ann Surg Oncol.* 1998;5(3):271–278.
- Liang J, Piao Y, Holmes L, et al. Neutrophils promote the malignant glioma phenotype through S100A4. *Clin Cancer Res.* 2014;20(1): 187–198.
- Kerber M, Reiss Y, Wickersheim A, et al. Flt-1 signaling in macrophages promotes glioma growth in vivo. *Cancer Res.* 2008; 68(18):7342–7351.
- Beck H, Raab S, Copanaki E, et al. VEGFR-1 signaling regulates the homing of bone marrow-derived cells in a mouse stroke model. *J Neuropathol Exp Neurol.* 2010;69(2):168–175.
- Gerber HP, Hillan KJ, Ryan AM, et al. VEGF is required for growth and survival in neonatal mice. *Development.* 1999;126(6): 1149–1159.
- Ferron M, Vacher J. Targeted expression of Cre recombinase in macrophages and osteoclasts in transgenic mice. *Genesis.* 2005; 41(3):138–145.
- Soriano P. Generalized lacZ expression with the ROSA26 Cre reporter strain. *Nat Genet.* 1999;21(1):70–71.
- Machein MR, Renninger S, Lima-Hahn E, Plate KH. Minor contribution of bone marrow-derived endothelial progenitors to the vascularization of murine gliomas. *Brain Pathol.* 2003;13(4):582–597.
- Rossiter H, Barresi C, Pammer J, et al. Loss of vascular endothelial growth factor activity in murine epidermal keratinocytes delays wound healing and inhibits tumor formation. *Cancer Res.* 2004; 64(10):3508–3516.
- Gerber HP, Malik AK, Solar GP, et al. VEGF regulates haematopoietic stem cell survival by an internal autocrine loop mechanism. *Nature.* 2002;417(6892):954–958.
- Jost MM, Ninci E, Meder B, et al. Divergent effects of GM-CSF and TGFbeta1 on bone marrow-derived macrophage arginase-1 activity, MCP-1 expression, and matrix metalloproteinase-12: a potential role during arteriogenesis. *FASEB J.* 2003;17(15): 2281–2283.
- Jacobs VL, Valdes PA, Hickey WF, De Leo JA. Current review of in vivo GBM rodent models: emphasis on the CNS-1 tumour model. *ASN Neuro.* 2011;3(3):e00063.
- Zagzag D, Miller DC, Chiriboga L, Yee H, Newcomb EW. Green fluorescent protein immunohistochemistry as a novel experimental tool for the detection of glioma cell invasion in vivo. *Brain Pathol.* 2003;13(1):34–37.
- Shojaei F, Zhong C, Wu X, Yu L, Ferrara N. Role of myeloid cells in tumor angiogenesis and growth. *Trends Cell Biol.* 2008;18(8): 372–378.
- Galdiero MR, Bonavita E, Barajon I, Garlanda C, Mantovani A, Jaillon S. Tumor associated macrophages and neutrophils in cancer. *Immunobiology.* 2013;218(11):1402–1410.
- Ferrara N. Vascular endothelial growth factor. *Arterioscler Thromb Vasc Biol.* 2009;29(6):789–791.
- Lin EY, Li JF, Gnatovskiy L, et al. Macrophages regulate the angiogenic switch in a mouse model of breast cancer. *Cancer Res.* 2006;66(13):11238–11246.
- Lin EY, Li JF, Bricard G, et al. Vascular endothelial growth factor restores delayed tumor progression in tumors depleted of macrophages. *Mol Oncol.* 2007;1(3):288–302.
- Ferrara N. Pathways mediating VEGF-independent tumor angiogenesis. *Cytokine Growth Factor Rev.* 2010;21(1):21–26.
- Baker GJ, Yadav VN, Motsch S, et al. Mechanisms of glioma formation: iterative perivascular glioma growth and invasion leads to tumor progression, VEGF-independent vascularization, and resistance to antiangiogenic therapy. *Neoplasia.* 2014;16(7): 543–561.
- Lucio-Eterovic AK, Piao Y, de Groot JF. Mediators of glioblastoma resistance and invasion during antivascular endothelial growth factor therapy. *Clin Cancer Res.* 2009;15(14):4589–4599.
- Ye XZ, Xu SL, Xin YH, et al. Tumor-associated microglia/macrophages enhance the invasion of glioma stem-like cells via TGF-beta1 signaling pathway. *J Immunol.* 2012;189(1): 444–453.
- Greenberg JI, Cheresch DA. VEGF as an inhibitor of tumor vessel maturation: implications for cancer therapy. *Expert Opin Biol Ther.* 2009;9(11):1347–1356.
- Greenberg JI, Shields DJ, Barillas SG, et al. A role for VEGF as a negative regulator of pericyte function and vessel maturation. *Nature.* 2008;456(7223):809–813.
- Stockmann C, Doedens A, Weidemann A, et al. Deletion of vascular endothelial growth factor in myeloid cells accelerates tumorigenesis. *Nature.* 2008;456(7223):814–818.
- Clausen BE, Burkhardt C, Reith W, Renkawitz R, Forster I. Conditional gene targeting in macrophages and granulocytes using LysMcre mice. *Transgenic Res.* 1999;8(4):265–277.
- Goldmann T, Wieghofer P, Muller PF, et al. A new type of microglia gene targeting shows TAK1 to be pivotal in CNS

- autoimmune inflammation. *Nat Neurosci.* 2013;16(11):1618–1626.
33. Prinz M, Priller J. Microglia and brain macrophages in the molecular age: from origin to neuropsychiatric disease. *Nat Rev Neurosci.* 2014;15(5):300–312.
34. Glass R, Synowitz M. CNS macrophages and peripheral myeloid cells in brain tumours. *Acta Neuropathol.* 2014;128(3):347–362.
35. Fantin A, Vieira JM, Gestri G, et al. Tissue macrophages act as cellular chaperones for vascular anastomosis downstream of VEGF-mediated endothelial tip cell induction. *Blood.* 2010;116(5):829–840.
36. Gabrusiewicz K, Ellert-Miklaszewska A, Lipko M, Sielska M, Frankowska M, Kaminska B. Characteristics of the alternative phenotype of microglia/macrophages and its modulation in experimental gliomas. *PLoS One.* 2011;6(8):e23902.
37. Galarneau H, Villeneuve J, Gowing G, Julien JP, Vallieres L. Increased glioma growth in mice depleted of macrophages. *Cancer Res.* 2007;67(18):8874–8881.